Supporting Information

Co-construction of sulfur vacancies and carbon confinement in V_5S_8/CNFs to induce an ultra-stable performance for half/full sodium-ion and potassium-ion batteries

Lihong Xu, [‡a] Xiaochuan Chen, [‡a, b] Wenti Guo, [e, f] Lingxing Zeng, *[a, d] Tao Yang, [g] Peixun Xiong, [c] Qinghua Chen,[a] Jianmin Zhang, *[e, f] Mingdeng Wei [c] and Qingrong Qian*[a, d]

[a] Engineering Research Center of Polymer Green Recycling of Ministry of Education, College of Environmental Science and Engineering, Fujian Normal University, Fuzhou, Fujian 35007, China. E-mail: zenglingxing@fjnu.edu.cn; qrqian@fjnu.edu.cn; Tel: +86 591 83465156.

[b] Key Laboratory for Polymeric Composite and Functional Materials of Ministry of Education, School of Chemistry, Sun Yat-Sen University, Guangzhou, China.

[c] Fujian Provincial Key Laboratory of Electrochemical Energy Storage Materials, Fuzhou University, Fuzhou, Fujian 350002, China.

[d] Key Laboratory of Advanced Energy Materials Chemistry (Ministry of Education), College of Chemistry, Nankai University, Tianjin 300071, China.

[e] Fujian Provincial Key Laboratory of Quantum Manipulation and New Energy Materials College of Physics and Energy, Fujian Normal University, Fuzhou, Fujian 350117, China. E-mail: jmzhang@fjnu.edu.cn; Tel: +86-591-22868141.

[f] Fujian Provincial Collaborative Innovation Center for Advanced High-Field Superconducting Materials and Engineering, Fuzhou, Fujian 350117, China.

[g] TEMA-NRG, Mechanical Engineering Department University of Aveiro, 3810-193 Aveiro, Portugal.

Experimental Section

Characterizations

The morphology of the composite was investigated by scanning electron microscopy (SEM, Hitachi 8100) and transmission electron microscopy (TEM, FEI F20 S-TWIN). X-ray diffraction (XRD) of the composite was performed by using a Bruker D8 diffractometer with Cu-Kα radiation operated in a range of diffraction angle 2θ from 10° to 80° at 40 kV and 40 mA. Raman spectroscopy (DXR2xi) was recorded with a wavelength of 532 nm laser radiation. X-ray photoelectron spectroscopy (XPS) was conducted on ESCALAB MARK II spectrometer by Kα radiation as the X-ray source. Thermal behavior of the composite during the heat treatment process was carried out by Thermal Gravimetric Analyzer (TA Q50) from 30°C to 700 °C with a heating rate of 10 °C min^{-1} in air flux of 100 mL min^{-1}. Electron paramagnetic resonance (EPR) experiment was collected with a JEOL JES-FA200 instrument. Elemental analysis (EA) was carried out by Vario EL cube.

Electrochemical Measurements

The electrochemical behaviors of the V_5S_8/CNFs for SIBs and PIBs were measured via CR2025-type coin cells at room temperature, which were all assembled in an argon-filled glovebox (O_2 ≤0.1 ppm, H_2O≤0.1 ppm).

To prepare the anode electrode for SIBs, active materials (V_5S_8/CNFs), super P and carboxymethyl cellulose sodium (CMC) at a weight ratio of 7:2:1 were mixed to form a homogeneous slurry. Subsequently, the above constituent was pasted onto copper foil with a diameter of 10 mm and dried at 80 °C for 10 h in vacuum overnight. The loading amount of active material on each copper foil was ca. 1-1.2 mg cm^{-2}. In the sodium-ion half-cells, sodium foil was used as the counter electrode, glass microfiber filter as separator, and 1M sodium perchlorate ($NaClO_4$) dissolved in ethylene carbonate (EC)/dimethyl carbonate (DMC) (1:1 by volume) with 5% fluorinated ethylene carbonate (FEC) as electrolyte. To prepare the cathode, 80 wt% active material ($Na_3V_2(PO_4)_3$), 10 wt% carbon black, and 10 wt% polyvinyldifluoride (PVDF) were blended using N-methyl-2-pyrrolidone (NMP) as solvent. Then, the slurry was uniformly coated on Al foil and subsequently cut into discs with diameter of 10 mm after drying under vacuum at 110 °C for 10 h. In the sodium ion full-cells, the V_5S_8/CNFs electrode and $Na_3V_2(PO_4)_3$ (NVP) electrode were utilized as anode and cathode (the mass ratio is about 1:5), respectively. The electrolyte and separator were the same as the above half-cells. Before testing, the half-cells were presodiated to achieve a stable surface/interface, which were first cycled between 0.01 and 3 V for 5 cycles and then discharged to a desired voltage. Then the as-prepared full cell was tested with a voltage range between 0.01 and 3.35 V. The specific capacity of the full cell was calculated based on the mass of anode.

For the PIBs, 70 wt% V_5S_8/CNFs, 20 wt% super-P and 10 wt% CMC were mixed, spreaded and dried on copper foil. The typical mass loading of active materials for each electrode sheets was ca. 1-1.2 mg cm^{-2}. 1 M potassium bis(fluoroslufonyl)imide (KFSI)-dimethoxyethane (DME) was employed as electrolyte. Potassium metal was served as the counter electrode and the separator was the same with the SIBs.

The electrochemical performance of the batteries was conducted on LAND CT2001A battery testing system at room temperature. Cyclic voltammetry (CV) curves with a desired sweep rate in the voltage window from 0.01 to 3.0 V were performed on an Ivium electrochemical workstation. Electrochemical impedance spectroscopies (EIS) was done on the same electrochemical workstation in the frequency range from 0.01 Hz to100 KHz.

First-principles calculations

Theoretical calculations were carried out by first-principles method based on density functional theory (DFT), as implemented in the Vienna ab initio Simulation Package (VASP).[S1] Projected augmented wave (PAW) potential and the Perdew-Burke-Ernzerhof (PBE) type generalized gradient approximation (GGA) were employed. The space group of V_5S_8 is C_2/m, which belongs to the monoclinic system.[S2,S3] The lattice constant of V_5S_8 is adopted according to ICSD with a = 11.399Å, b = 6.668Å and c = 11.311Å.[16,17] The Brillouin zone of the V_5S_8 supercell is sampled using a 4 × 5 × 4 k-mesh under the Monkhorst-Pack method. The cut-off energy of the plane wave expansion of the electron wave function is set to 400 eV. Through the conjugate gradient (CG) algorithm, all the atoms in each unit cell are completely relaxed until the residual force on each atom is less than 0.02 eV/Å. Minimum energy pathway (MEP) and the activation energy for K diffusion are calculate using the climbing image nudged elastic band (CI-NEB) method.[S4]

Supplementary Figures and Tables

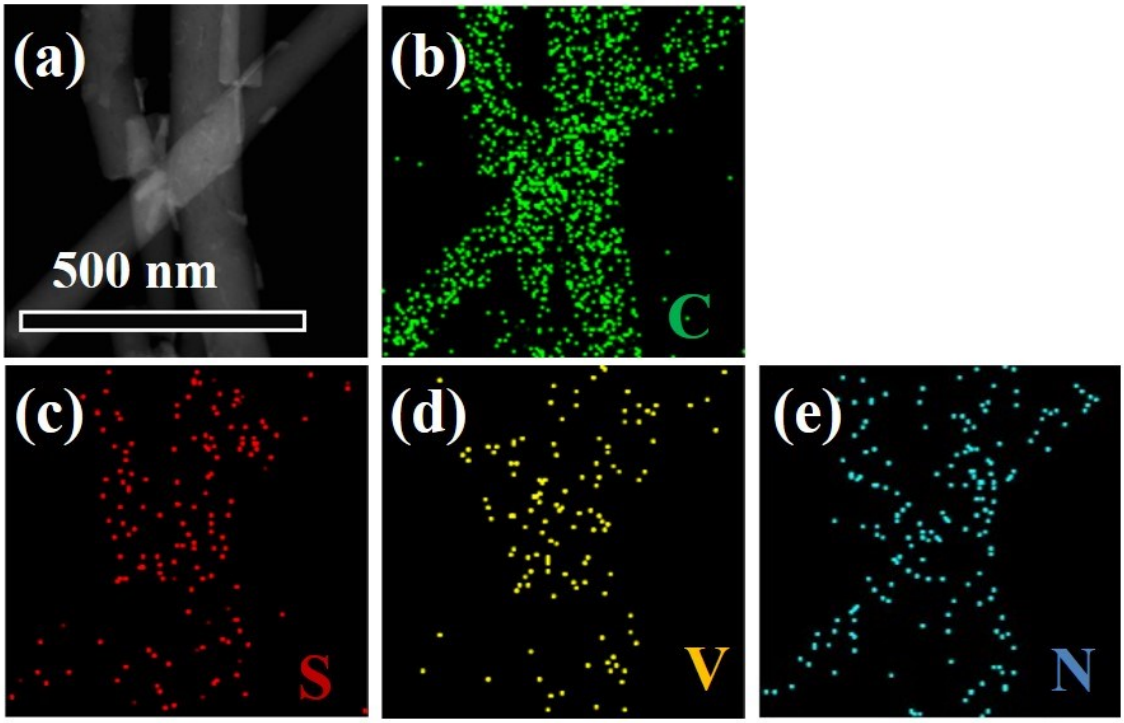

Fig. S1. STEM-EDS element mappings for C, V, S and N of the D-V_5S_8/CNFs composite.

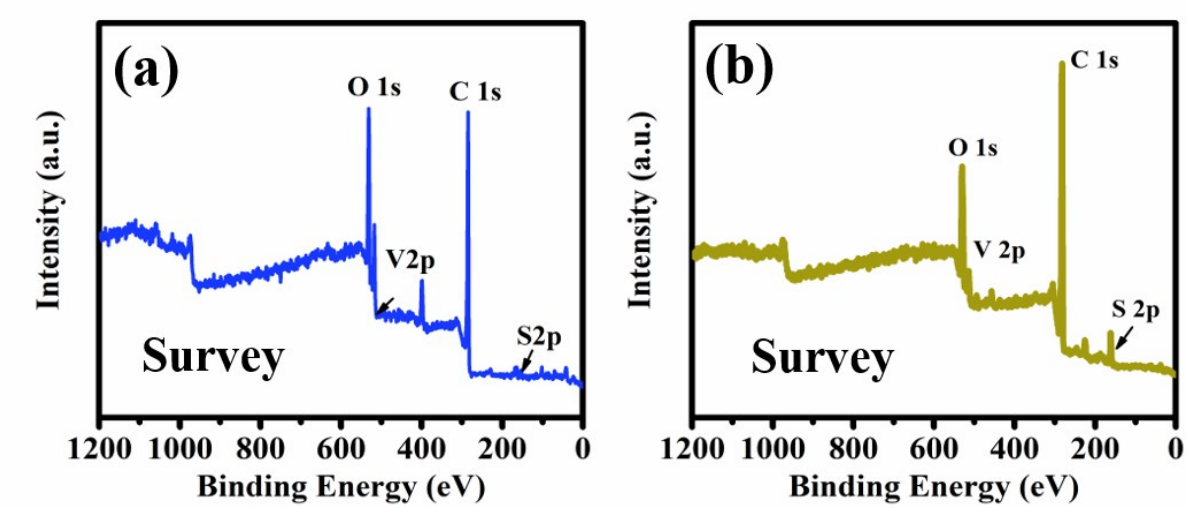

Fig. S2 Survey XPS spectra of (a) D-V_5S_8/CNFs and (b) P-V_5S_8/C samples.

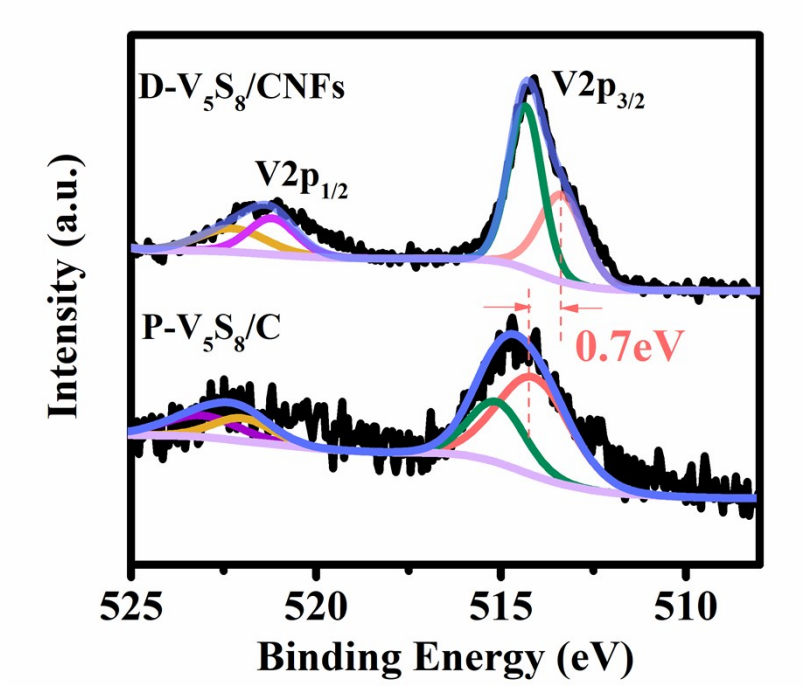

Fig. S3 V 2p XPS spectra of (a) D-V_5S_8/CNFs and (b) P-V_5S_8/C samples.

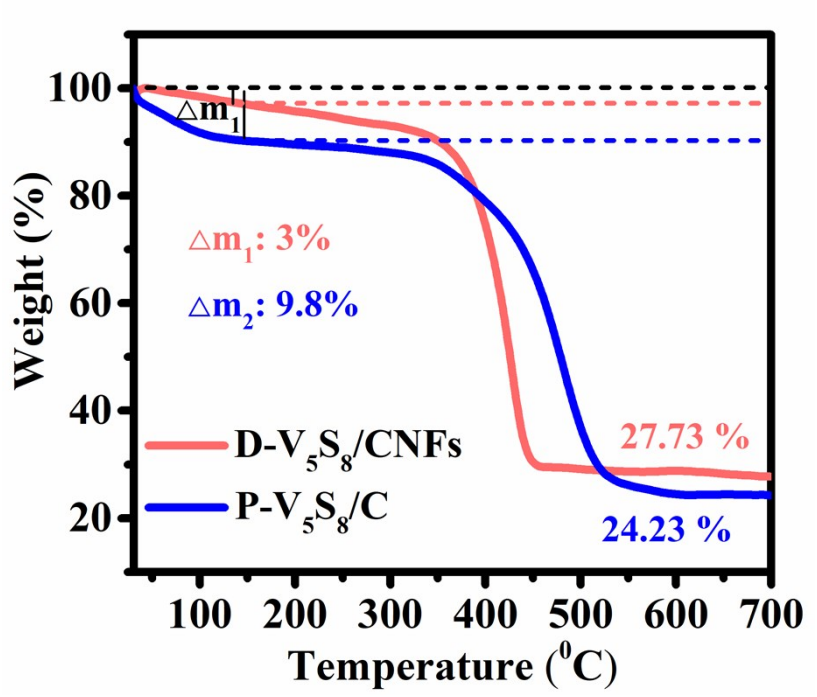

Fig. S4 TG-DSC curve of D-V_5S_8/CNFs and P-V_5S_8/C composites.

TGA-DSC measurements is achieved in Air atmosphere to determine the V_5S_8 contents in D-V_5S_8/CNFs and P-V_5S_8/C composites. For example, in D-V_5S_8/CNFs, a narrow dip (3%) before 150 °C is corresponded to the evaporation of absorbed water. And then an abruptly weight loss can be clearly observed from 150 to 700 °C, which can be ascribed to the carbon completely burned off in air and V_5S_8 oxidized to V_2O_5 finally. The loading content of V_5S_8 in the final product D-V_5S_8/CNFs and P-V_5S_8/C composites are around 32.1 wt% and 30.1 wt%, respectively.[21,33,38]

$2V_5S_8 + 57/2O_2 \rightarrow 5V_2O_5 + 16SO_2$

For D-V_5S_8/CNFs, the V_5S_8 content (V_5S_8 wt%) can be calculated as

V_5S_8 (□□%) = 100%×2/5×(M_{V5S8}/M_{V2O5}) × ($W_{remain\ V2O5}$ / $W_{150°}$) = 100% × 2/5 × (510.7/181.88) × (27.73) /97%=32.1%

For P-V_5S_8/C, the V_5S_8 content (V_5S_8 wt%) can be calculated as

V_5S_8 (□□%)=100%×2/5×(M_{V5S8}/M_{V2O5}) × ($W_{remain\ V2O5}$ / $W_{150°}$) = 100% × 2/5 × (510.7/181.88) ×(24.23) /90.2%=30.1%

$W_{150°}$: The weight retained at the temperature of 150°C.

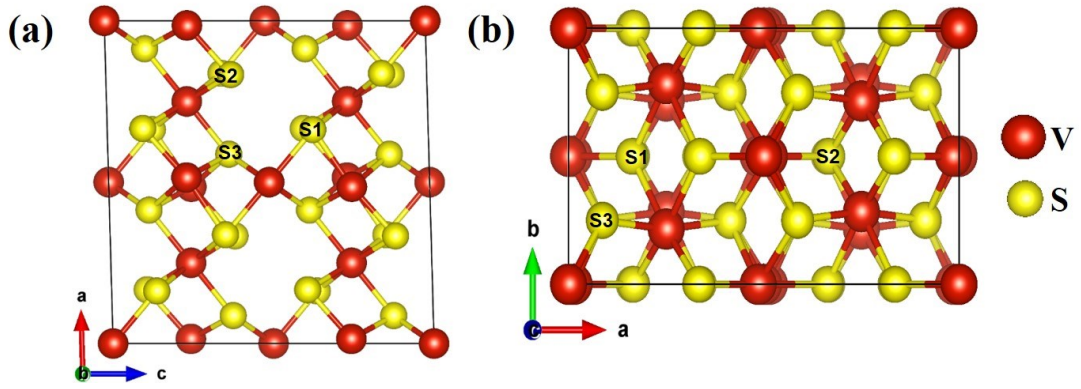

Fig. S5 (Color online) Schematic illustration of the atom arrangements in V_5S_8. (a) side view; and (b) top view of the crystal structure.

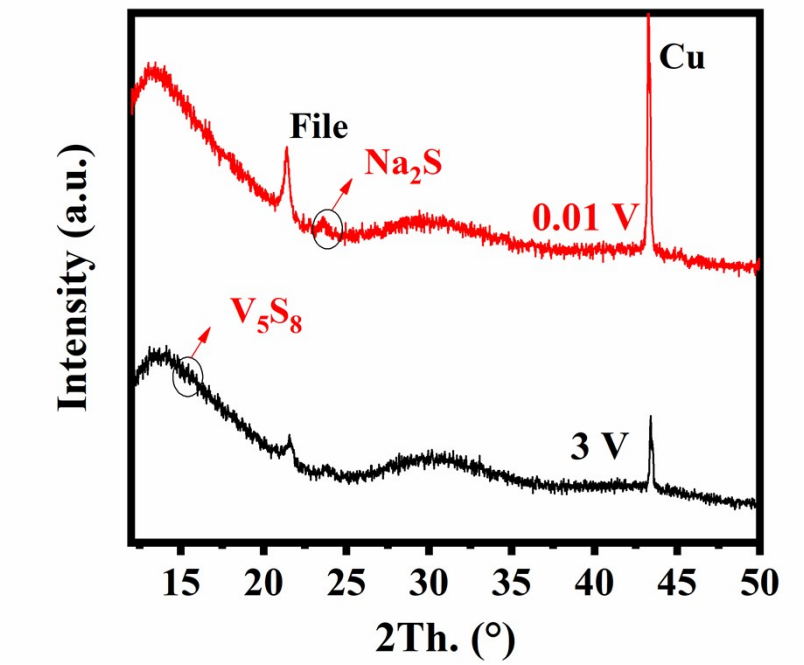

Fig. S6 Ex-situ XRD patterns of D-V_5S_8/CNFs electrode after discharging to 0.01 V and finally charging to 3 V at 0.1 A g^{-1}.

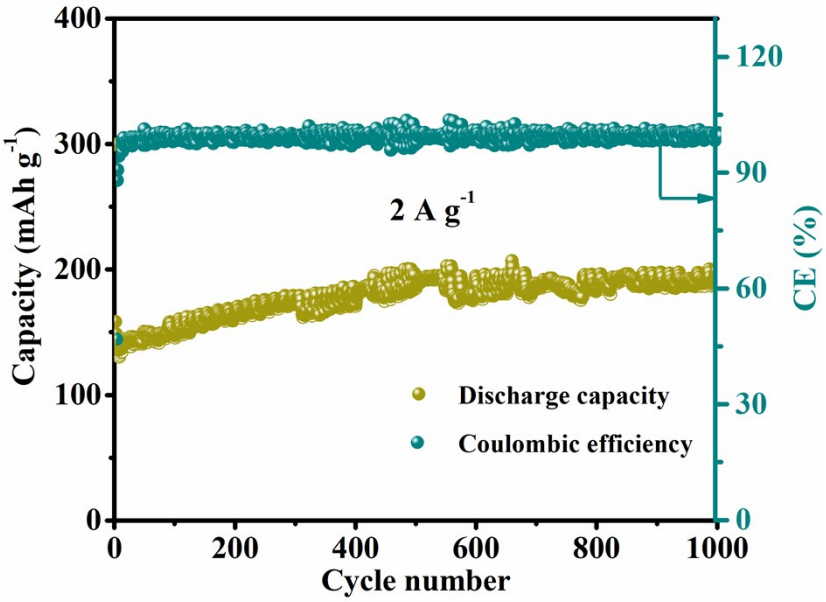

Fig. S7 Long-term cycling performance and Coulombic efficiency at 2 A g^{-1} of P-V_5S_8/C electrode in SIBs.

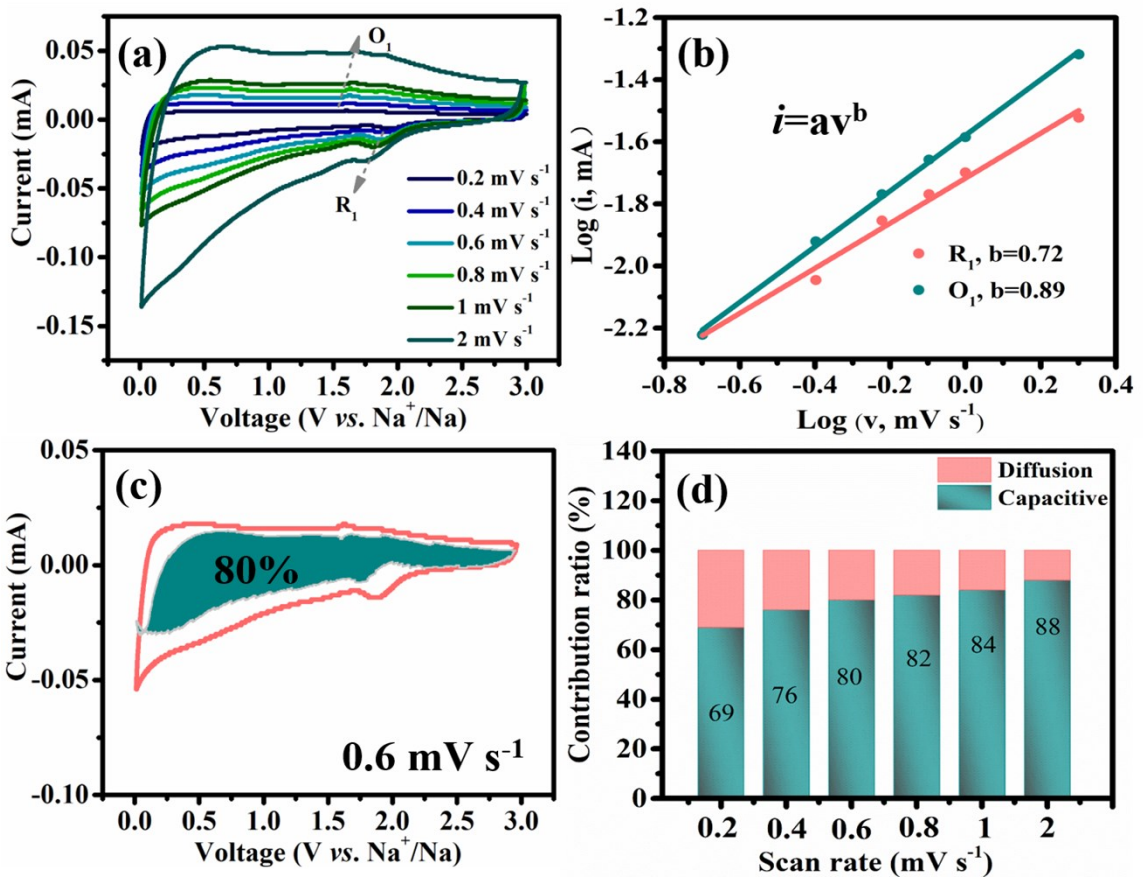

Fig. S8 Quantitative analysis of surface-dominated behavior in D-V_5S_8/CNFs electrode for SIBs. (a) Cyclic voltammetry curves at various scan rates of 0.2 to 2 mV s^{-1}. (b) b value determination. (c) Contribution percentages of capacitive (blue area) at 0.6 mV s^{-1}. (d) Contribution percentages of diffusion (red) and capacitance (blue) at different rates.

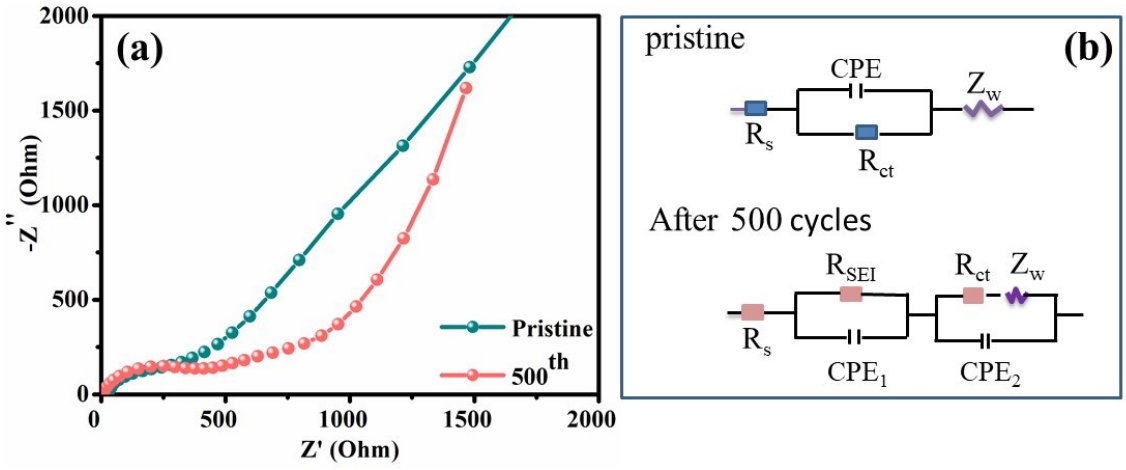

Fig. S9 (a) The Nyquist plots and (b) equivalent circuit model of D-V_5S_8/CNFs electrode before cycling and after 500 cycles at 2 A g^{-1} for SIBs.

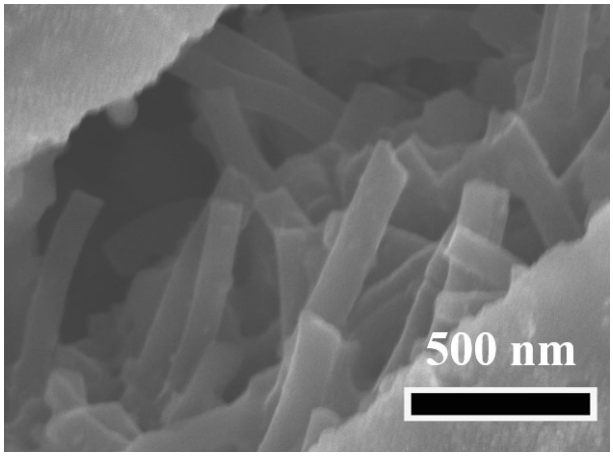

Fig.S10 The SEM image of D-V_5S_8/CNFs electrode after 1000 cycles at 1 A g^{-1} for SIBs.

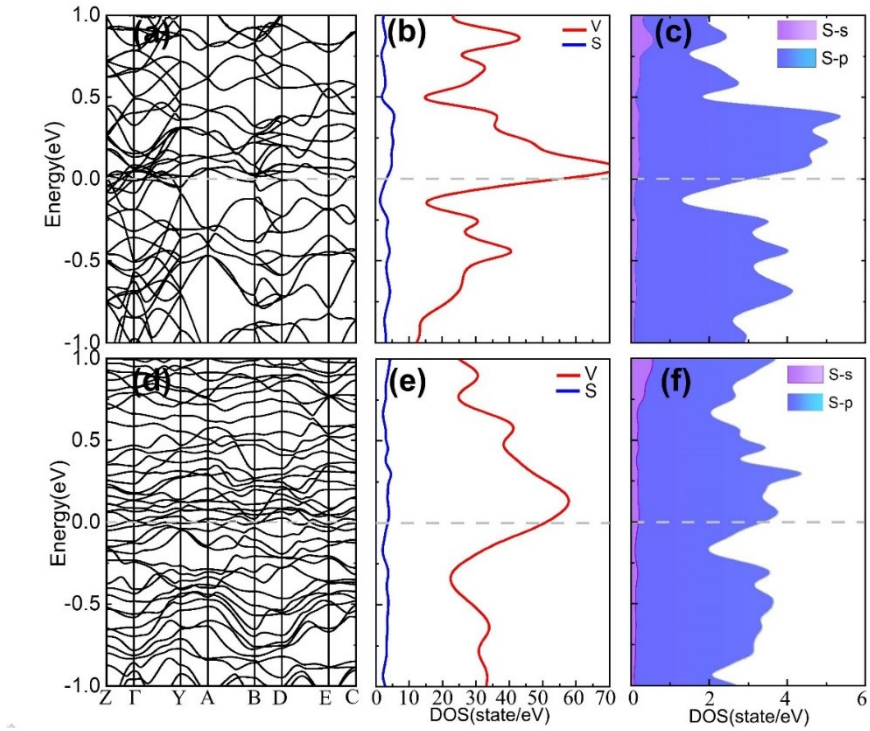

Fig. S11 The columns from left to right are the band structure, the total density of states of S and V, and the partial density of states of S and V in perfect V_5S_8 (a, b, c), and S-defective V_5S_8 (d, e, f), respectively. The gray dashes in the Figures represent the Fermi level.

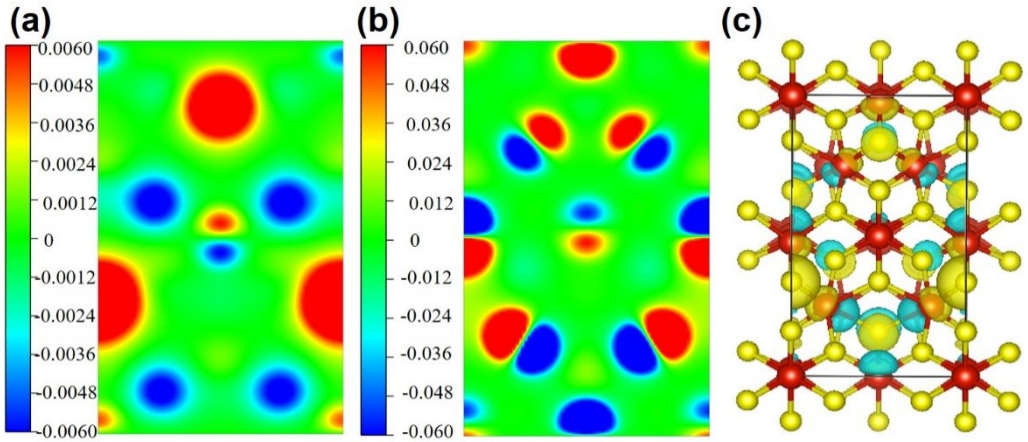

Fig. S12 The distances from the XOY plane are (a) 0 * d and (b) 0.75 * d; (c) Structure hockey view.

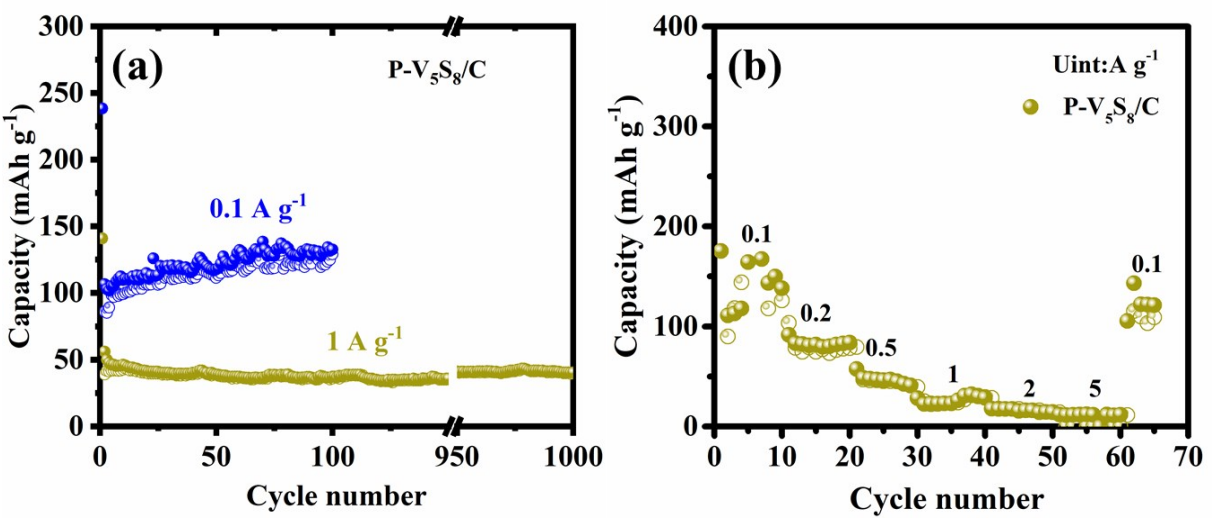

Fig. S13 (a) Cycling performance of P-V_5S_8/C electrode at 0.1A and 1 A g^{-1}. (b) Rate capability of P-V_5S_8/C electrode under various current densities from 0.1 A g^{-1} to 5 A g^{-1} in PIBs.

Table S1. Elemental analysis results from D-V_5S_8/CNFs

Element	C (wt.%)	S (wt.%)	N (wt.%)	H (wt.%)
Content	41.14	10.28	10.19	4.65

Table S2 Calculated formation Energy for V_5S_8 with vacancy defect (S1, S2 and S3).

Configuration	E_f (eV)
S1	-351.25
S2	-351.54
S3	-351.37

Table S3 Electrochemical performance comparison of the D-V_5S_8/CNFs with other sulfide anode materials for SIBs/PIBs.

Electrode Materials	Fields	Current density ($A\ g^{-1}$)	Cycling capacity/ ($mAh\ g^{-1}$)	Cycles	Year/Ref.
V_5S_8@C	PIBs	2	190	1000	2019/[S5]
V_5S_8-graphite	SIBs	1	496	500	2017/[S6]
V_3S_4@C	SIBs	1	150	4000	2020/[S7]
	PIBs	1	182	4000	
V_3S_4@NCNFs	PIBs	2	245	1000	2020/[S8]
VS_2 nanosheets	SIBs	1	500	200	2017/[S9]
	PIBs	0.5	360	100	
VS_2-SNSs	SIBs	5	204	600	2017/[S10]
VS_4-rGO	SIBs	0.5	402	300	2018/[S11]
FeS_2@C	SIBs	10	220	10000	2020/[S12]
SnS_2/Graphen	PIBs	0.1	559	50	2019/[S13]
CuS@CoS_2	SIBs	0.5	≈400	500	2019/[S14]
D-V_5S_8/CNFs	**SIBs**	**5**	**190**	**17000**	**This work**
	PIBs	**1**	**165**	**3000**	

Table S4 Impedance parameters calculated from an equivalent circuit model.

Sample	R_s (Ω)	R_{ct} (Ω)	R_{SEI}
Pristine	28.37	205.9	
500^{th}	15.55	175.2	301.4

REFERENCES

[S1] Z. Hong, Y. Zhen, Y. Ruan, M. Kang, K. Zhou, J. M. Zhang, Z. Huang and M. Wei, *Adv. Mater.,* 2018, **30**, 1802035.

[S2] P. E. BlÖchl, *Phys. Rev. B,* 1994, **50**, 17953.

[S3] J. P. Perdew, K. Burke, M. Ernzerhof, *Phys. Rev. Lett.,* 1996, **77**, 3865.

[S4] G. Henkelman, H. Jónsson, *J. Chem. Phys.*, 2000, **113**, 9978-9985.

[S5] L. Li, W. Zhang, X. Wang, S. Zhang, Y. Liu, M. Li, G. Zhu, Y. Zheng, Q. Zhang, T. Zhou, W. K. Pang, W. Luo, Z. Guo and J. Yang, *ACS Nano,* 2019, **13**, 7939-7948.

[S6] C. Yang, X. Ou, X. Xiong, F. Zheng, R. Hu, Y. Chen, M. Liu and K. Huang, *Energy Environ. Sci.*, 2017, **10**, 107-113.

[S7] Y. Liu, Z. Sun, X. Sun, Y. Lin, K. Tan, J. Sun, L. Liang, L. Hou and C. Yuan, *Angew. Chem. Int. Ed.,* 2020, **59**, 2473-2482.

[S8] D. Wu, W. Zhang, Y. Feng and J. Ma, *J. Mater. Chem. A,* 2020, **8**, 2618-2626.

[S9] J. Zhou, L. Wang, M. Yang, J. Wu, F. Chen, W. Huang, N. Han, H. Ye, F. Zhao, Y. Li and Y. Li, *Adv. Mater.*, 2017, **29**, 1702061.

[S10] R. Sun, Q. Wei, J. Sheng, C. Shi, Q. An, S. Liu and L. Mai, *Nano Energy*, 2017, **35**, 396-404.

[S11] S. Wang, F. Gong, S. Yang, J. Liao, M. Wu, Z. Xu, C. Chen, X. Yang, F. Zhao, B. Wang, Y. Wang and X. Sun, *Adv. Funct. Mater.,* 2018, **28**, 1801806.

[S12] Z. Man, P. Li, D. Zhou, Y. Wang, X. Liang, R. Zang, P. Li, Y. Zuo, Y. M. Lam and G. Wang, *Nano Lett.,* 2020, **20**, 3769-3777.

[S13] D. S. Bin, S. Y. Duan, X. J. Lin, L. Liu, Y. Liu, Y. S. Xu, Y. G. Sun, X. S. Tao, A. M. Cao and L. J. Wan, *Nano Energy,* 2019, **60**, 912-918.

[S14] Y. Fang, B. Y. Guan, D. Luan and X. W. Lou, *Angew. Chem. Int. Ed.,* 2019, **58**, 7739-7743.